

# Activation Energy of Methyl Radical Decay in Methane Hydrate

Kei Takeya, Kouhei Nango, Takeshi Sugahara, and Kazunari Ohgaki\*

Division of Chemical Engineering, Graduate School of Engineering Science, Osaka University, Toyonaka, Osaka 560-8531, Japan

Atsushi Tani

Department of Earth and Space Science, Graduate School of Science, Osaka University, Toyonaka, Osaka 560-0043, Japan

Received: July 21, 2005; In Final Form: September 13, 2005

The thermal stability of  $\gamma$ -ray-induced methyl radicals in methane hydrate was studied using the ESR method at atmospheric pressure and 210–260 K. The methyl radical decay proceeded with the second-order reaction, and ethane molecules were generated from the dimerization process. The methyl radical decay proceeds by two different temperature-dependent processes, that is, the respective activation energies of these processes are  $20.0 \pm 1.6$  kJ/mol for the lower temperature region of 210–230 K and  $54.8 \pm 5.7$  kJ/mol for the higher temperature region of 235–260 K. The former agrees well with the enthalpy change of methane hydrate dissociation into ice and gaseous methane, while the latter agrees well with the enthalpy change into liquid water and gaseous methane. The present findings reveal that methane hydrates dissociate into liquid (supercooled) water and gaseous methane in the temperature range of 235–260 K.

## Introduction

Clathrate hydrates have a curious icy structure composed of hydrogen bonds. This structure consists of many cages that include guest gas molecules. The wholly empty clathrate has not been observed in nature, but the structure can be stabilized by inclusion of a second component, the guest species.<sup>1</sup> The clathrate hydrate including methane molecules is called methane hydrate, and has a cubic unit cell, structure I. Structure I is generated by molecules of 0.4–0.6 nm in diameter, such as methane.

Clathrate hydrates have attracted much attention as new materials because of their unique structure and properties, such as high compression of gaseous molecules. Methane hydrates have been studied by various researchers using Raman spectroscopy<sup>2</sup> and X-ray diffraction<sup>3</sup> for investigation of hydrate stability, dissociation process, and cage occupancy. An electron spin resonance (ESR) investigation of clathrate hydrates was reported by Trofimov et al., who studied radicals in  $\gamma$ -irradiated hydrates of three-membered cycles.<sup>4</sup> Nonetheless, the irradiation effects of clathrate hydrates and thermal stability of radicals induced in hydrate have not been examined sufficiently.

In a previous study, we reported the generation of methyl radicals and their decay at 210–230 K from the ESR analysis of  $\gamma$ -ray-irradiated methane hydrate, where the decay of the methyl radicals appeared to follow the dissociation of methane hydrate.<sup>5</sup> As a further examination of the stability of the radical and its relation to the dissociation of methane hydrate, we here report the details of the radical decay in  $\gamma$ -ray-irradiated methane hydrate in the higher temperature region of 235–260 K.

## Experimental Section

**Sample Preparation.** Methane hydrate was synthesized at ca. 5–10 MPa and a slightly lower temperature (277–279 K)

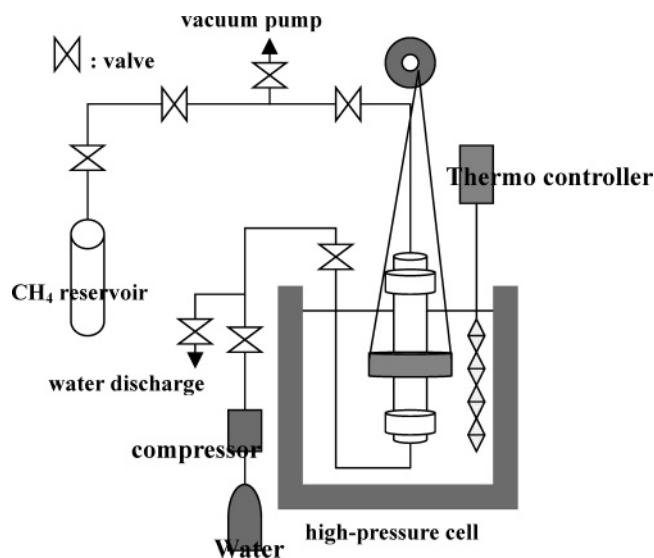


Figure 1. Schematic illustration of the experimental setup.

than that of the equilibrium state in a high-pressure cell made of stainless steel. A schematic illustration of the experimental setup used in this study is shown in Figure 1. Methane and deionized water were introduced into the high-pressure cell and mixed using a magnetic stirrer. The system temperature was controlled by thermostated water circulating from a thermo-controller (TRL117C, THOMAS). The system pressure was measured by a pressure gauge (VSMC series, VALCOM). After the gas and the water had been stirred, methane hydrate was obtained from the stainless pressure cell at ca. 253 K in a low-temperature chamber. The samples were small pieces with diameters of 1–2 mm.

Hydrate particles of about 1 mm in diameter were picked up and kept in a plastic vial called a cryovial. The vials were immersed in liquid nitrogen during  $\gamma$ -ray irradiation at a dose

\* To whom correspondence should be addressed. Tel: +81-6-6850-6290. Fax: +81-6-6850-6290. E-mail: ohgaki@cheng.es.osaka-u.ac.jp.

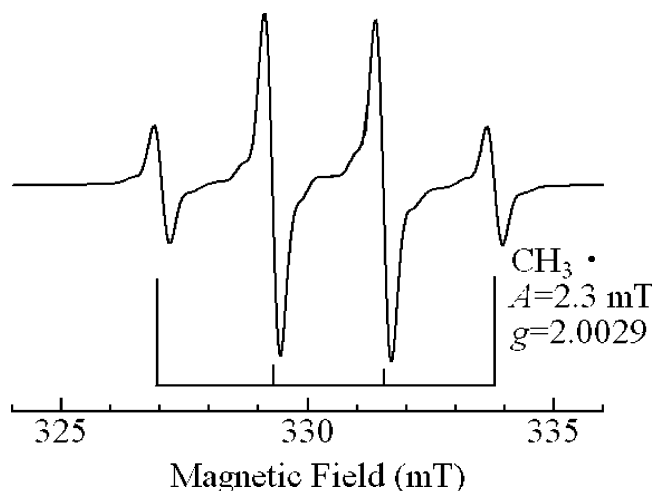


Figure 2. ESR spectrum of the induced methyl radicals.

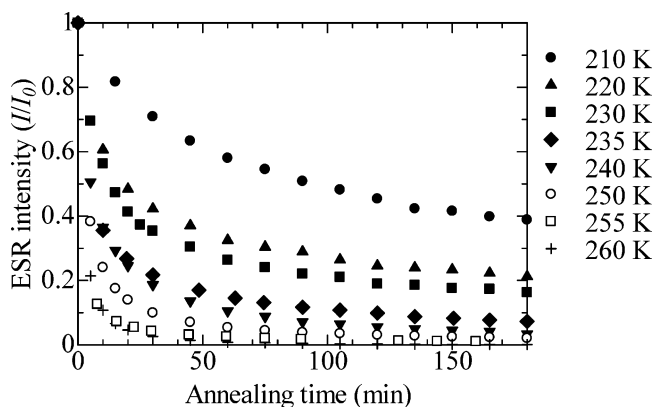


Figure 3. Isothermal annealing curves of the methyl radicals at 210–260 K.

of 10 kGy using a source of  $^{60}\text{Co}$ . Several pieces about 5 mg were set in the ESR sample tube at 77 K. Liquid oxygen and nitrogen in the tube were removed by careful evacuation.

**ESR Measurements.** The polycrystalline samples were measured at 210–260 K, which is the same as the annealing temperature, by an X-band commercial ESR spectrometer (JEOL RE1X) with 100 kHz field modulation of 0.1 mT and microwave power of 1 mW using a nitrogen gas flow unit system (JEOL ES-DVT2). In isothermal annealing experiments, the sample was measured every 15 min of heating at temperatures of 210, 220, 230, 235, 240, 250, 255, and 260 K. The signal intensity was determined by the peak amplitude of the ESR spectrum, since the line shape did not change throughout the measurements.

## Results and Discussion

Figure 2 shows the ESR spectrum of the methyl radicals. The isothermal annealing curves for the methyl radicals at 210, 220, 230, 235, 240, 250, 255, and 260 K are shown in Figure 3. Their ESR intensity was normalized by the initial intensity on the vertical axis.

There are, in general, two types of decay kinetics of radical species: the first- and second-order annealing models. In this study, the decay model of the methyl radicals appeared to follow the second-order model at 210–260 K, because the annealing curves fit well to the second-order model (Figure 4a) rather than the first-order one following the simple exponential decay curve (Figure 4b). The second-order decay rate ( $dI/dt$ ) depends on the square of the radical density and requires the reciprocal

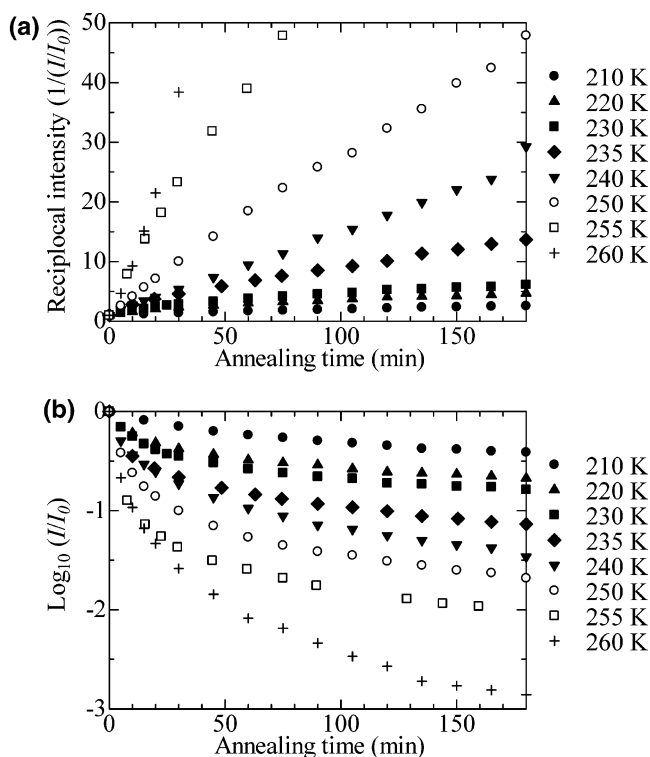


Figure 4. (a) Isothermal annealing curves for the methyl radicals plotted as reciprocal intensities. (b) Isothermal annealing curves for the methyl radicals plotted in a semilogarithmic form.

density to be in proportion to the annealing time. This process is written as

$$-dI/dt = \lambda I^2 \propto \lambda n^2$$

or

$$1/I = 1/I_0 + \lambda t$$

where  $I$  is the signal intensity of ESR spectra for the methyl radicals,  $I_0$  is the initial intensity, and  $\lambda$  is the rate constant for the second-order kinetics. The second-order decay model suggests that ethane is generated in the decay process through the dimerization reaction of the methyl radicals. With the exception of the peak for methane, only a single additional peak, corresponding to ethane, was detected by gas chromatography after wholly dissociating the  $\gamma$ -irradiated methane hydrate. The above finding also supports the second-order decay model.

This rate constant is described by the following Arrhenius' equation

$$1/\lambda = (1/\lambda_0)\exp(E/k_B T)$$

where  $\lambda_0$  is the frequency factor,  $E$  is the activation energy, and  $k_B$  is the Boltzmann constant.

From the Arrhenius plot for the methyl radicals shown in Figure 5, the methyl radical decay in methane hydrate has two different activation energies depending on the temperatures. The activation energy is  $20.0 \pm 1.6$  kJ/mol in the low-temperature region of 210–230 K and  $54.8 \pm 5.7$  kJ/mol in the high-temperature region of 235–260 K. The variation in the literature values of enthalpy change of dissociation for methane hydrate is listed in Table 1. These values are 18.13, 19.06, and 23.37 kJ/mol for hydrate dissociation into ice and gas and 54.19, 54.36, and 67.85 kJ/mol for hydrate dissociation into water and gas.

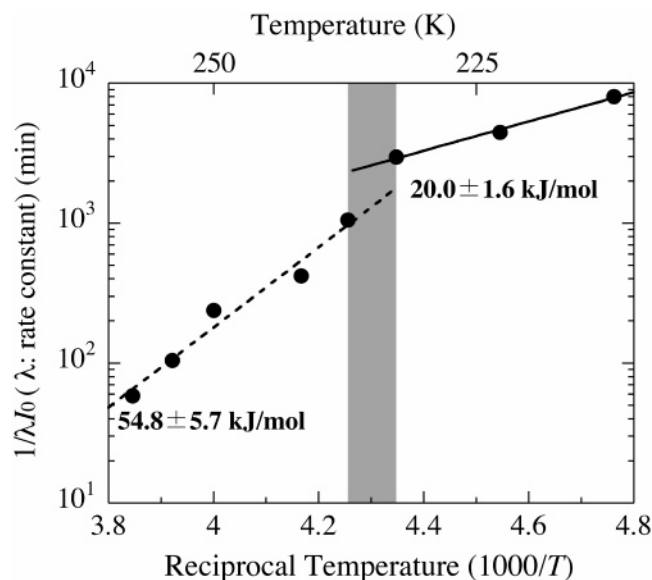


**Figure 5.** Arrhenius plot for the parameters  $\lambda$  and  $I_0$  of the second-order annealing obtained from the isothermal annealing experiments. The slope of the fitting line gives the activation energy  $E$ . There is a change of the rate constant between 230 and 235 K, indicated by gray shading.

**TABLE 1: Enthalpy Changes  $\Delta H$  of the Dissociation of Methane Hydrate (hydrate = ice + gas) (hig), (hydrate = water + gas) (hlg), and Activation Energy  $E$  for the Methyl Radicals**

$\Delta H$ (kJ/mol) literature	$E$ (kJ/mol) this work	temperature region
$\Delta H$ (hig) 18.13, <sup>6</sup> 19.06, <sup>7</sup> 23.37 <sup>8</sup>	$20.0 \pm 1.6$	210–230 K
$\Delta H$ (hlg) 54.19, <sup>6</sup> 54.36, <sup>9</sup> 67.85 <sup>8</sup>	$54.8 \pm 5.7$	235–260 K

The activation energy of the methyl radical decay agrees well with the enthalpy change of hydrate dissociation.

Induced methyl radicals are trapped and isolated in cages, because these radicals did not decay over several months at 77 K. Since radical decay was apparently observed in the unstable region, these radicals cannot migrate through the cage structure. The methyl radicals released from hydrate cages are simultaneously dimerized to generate ethane molecules during hydrate structure dissociation. Therefore, the activation energy of radical decay corresponds to the enthalpy change of hydrate dissociation in the low-temperature region.

In the high-temperature region, the activation energy of radical decay corresponds to the enthalpy change of hydrate dissociation into water and methane. It is quite interesting that methane hydrate dissociation at a temperature higher than 235 K produces liquid supercooled water instead of solid ice. In other words, the methyl radicals are not decayed with the energy of hydrate dissociation into ice and methane. According to the above hypothesis, we can estimate the hydration number,  $n$ , described by  $\text{CH}_4 \cdot n\text{H}_2\text{O}$

$$n = (E(\text{hlg}) - E(\text{hig})) / \Delta H(\text{melt})$$

where  $\Delta H(\text{melt})$  is the enthalpy change of water fusion (liquid

to ice), 6.0 kJ/mol. The calculated hydration number is  $5.8 \pm 1.2$ , which is very close to the ideal hydration number of the structure I hydrate crystal, 5.75. According to Langham,<sup>10</sup> the lower stability boundary of supercooled water is near 235 K. These facts support the notion that the methane hydrate dissociation above 235 K generates supercooled water instead of ice.

The most important findings in the present study are as follows:

1. The methyl radical decay in the methane hydrate proceeds with the second-order reaction (dimerization of methyl radicals) and produces the ethane molecule.
2. The activation energy of methyl radical decay jumps from  $E(\text{hig})$  to  $E(\text{hlg})$  at a turning point which is located between 230 and 235 K.
3. Each activation energy corresponds to the enthalpy change of methane hydrate dissociation. This fact suggests that methane hydrate dissociation generates supercooled water instead of ice in the temperature region of 235–260 K.

## Conclusion

The methyl radical in  $\gamma$ -irradiated methane hydrate, which is decayed to produce the ethane molecule through the second-order reaction, has two different activation energies for the decay process,  $20.0 \pm 1.6$  kJ/mol for 210–230 K and  $54.8 \pm 5.7$  kJ/mol for 235–260 K. The activation energy of 20.0 kJ/mol is nearly equal to the enthalpy change of methane hydrate dissociation into ice and methane, while 54.8 kJ/mol corresponds to the dissociation into supercooled water and methane.

**Acknowledgment.** We thank Drs. H. Sato, C. Yamanaka, and M. Katsura for their helpful input. We are indebted to Dr. T. Ikeda at the Institute of Scientific and Industrial Research of Osaka University for  $^{60}\text{Co}$   $\gamma$ -ray irradiation. K.T. thanks the 21st Century Center of Excellence (COE) Program, “Creation of Integrated EcoChemistry”. We are also grateful to Professor T. Kasai (a cooperative research member of COE) for his valuable suggestions. This study was partly supported by a Grant-in-Aid for Scientific Research from the Japanese Ministry of Education, Culture, Sports, Science and Technology (No. 15750008).

## References and Notes

- (1) van der Waals, J. H.; Plateeuw, J. C. *Adv. Chem. Phys.* **1959**, 2, 1.
- (2) Nakano, S.; Moritoki, M.; Ohgaki, K. *J. Chem. Eng. Data* **1999**, 44, 4 (2), 254.
- (3) Takeya, S.; Ebinuma, T.; Uchida, T.; Nagao, J.; Narita, H. *J. Cryst. Growth* **2002**, 237–239, 379.
- (4) Trofimov, V. I.; Blumenfeld, A. L.; Kostyanovsky, R. G.; Chkheidze, I. I. *Tetrahedron Lett.* **1971**, 35, 3267.
- (5) Takeya, K.; Tani, A.; Yada, T.; Ikeya, M.; Ohgaki, K. *Jpn. J. Appl. Phys.* **2004**, 43 (1), 353.
- (6) Handa, Y. P. *J. Chem. Thermodyn.* **1986**, 18, 915.
- (7) Frost, E. M., Jr.; Deaton, W. M. *Oil Gas J.* **1946**, 45 (12), 170.
- (8) De Roo, J. L.; Peters, C. J.; Lichtenthaler, R. N.; Diepen, G. A. M. *AIChE J.* **1983**, 29, 9 (4), 651.
- (9) Roberts, O. L.; Brownscombe, E. R.; Howe, L. S.; Ramser, H. *Pet. Manage.* **1941**, 12 (6), 56, 58–60, 62.
- (10) Langham, E. J.; Mason, B. J. *Proc. R. Soc. London* **1958**, A247, 493.